

Nematic and time-reversal breaking superconductivities coexisting with quadrupole order in a Γ_3 system

Katsunori Kubo

Advanced Science Research Center, Japan Atomic Energy Agency, Tokai, Ibaraki 319-1195, Japan

(Dated: February 26, 2020)

We discuss superconductivity in a model on a cubic lattice for a Γ_3 non-Kramers system. In previous studies, it is revealed that d -wave superconductivity with E_g symmetry occurs in a wide parameter range in a Γ_3 system. Such anisotropic superconductivity can break the cubic symmetry of the lattice. In a Γ_3 system, the quadrupole degrees of freedom are active and the effect of the cubic symmetry breaking should be important. Here, we investigate the coexisting states of the d -wave superconductivity and quadrupole order by a mean-field theory. In particular, we discuss possible competition and cooperation between the superconductivity and quadrupole order depending on types of them. We find nematic superconductivity breaking the cubic symmetry and coexisting with quadrupole order. In the present model, we also find $d + id$ superconductivity, which breaks time-reversal symmetry but retains the cubic symmetry. We also discuss the effects of uniaxial stress on these superconducting states.

I. INTRODUCTION

In the vicinity of antiferromagnetically ordered phases, superconductivity is often found such as in cuprate high-temperature superconductors^{1,2}, in Fe-based superconductors^{3,4}, and in heavy-fermion materials^{5,6}. Superconductivity in these materials cannot be explained by the conventional phonon-mediated pairing mechanism, and they are called unconventional superconductors^{7,8}. The mechanism of the unconventional superconductivity in these materials has been a central issue in condensed matter physics. In particular, the spin-fluctuation-mediated superconducting mechanism has been widely discussed.

In addition, the orbital degrees of freedom may also play key roles in the superconductivity of orbitally degenerate systems. The importance of the orbital degrees of freedom was suggested for f -electron superconductors⁹⁻¹². For the Fe-based superconductors, the importance of the orbital fluctuations has also been discussed^{13,14}. Then, the interplay between the spin and orbital degrees of freedom became an important issue in the field of the unconventional superconductivity.

It is also interesting to explore possibility of unconventional superconductivity without spin degrees of freedom. For this purpose, an f -electron system with the Γ_3 non-Kramers doublet state under a cubic crystalline electric field (CEF) is a plausible candidate. The Γ_3 state has the same symmetry as the spinless e_g electron and possesses quadrupole and octupole moments but does not have the dipole moment. Thus, the Γ_3 system can be regarded as an ideal system to investigate orbital physics and there may be a route to unconventional superconductivity other than the spin fluctuation mechanism.

In actual Γ_3 systems, superconductivity has been reported in $\text{PrT}_2\text{X}_{20}$ (T = transition metal element, X = Zn, Al). In this series of compounds, the CEF ground state of the f^2 electronic configuration in a Pr^{3+} ion is the Γ_3 doublet¹⁵⁻²³ (strictly, in $\text{PrRh}_2\text{Zn}_{20}$, the CEF ground state is the Γ_{23} doublet due to symmetry lowering at the Pr site induced by a structural transi-

tion²²). In these materials, quadrupole order often realizes and the relation between the superconductivity and the quadrupole degrees of freedom has been discussed. In $\text{PrIr}_2\text{Zn}_{20}$ ^{16,19,24,25} and $\text{PrV}_2\text{Al}_{20}$ ^{18,26}, superconductivity takes place below the antiferroquadrupole (AFQ) ordering temperature T_{AFQ} . For $\text{PrIr}_2\text{Zn}_{20}$, the order parameter of the AFQ ordering is determined to be $O_2^2 = x^2 - y^2$ ²⁵. On the other hand, superconductivity takes place below the ferroquadrupole (FQ) ordering temperature T_{FQ} in $\text{PrTi}_2\text{Al}_{20}$ ^{15,18,20,27-31}. The order parameter of the FQ ordering in this compound is determined to be $O_2^0 = 3z^2 - r^2$ ^{20,31}. In $\text{PrRh}_2\text{Zn}_{20}$, superconductivity occurs simultaneously with AFQ ordering^{21,32}.

To develop a theory for the Γ_3 systems, we have constructed models for f electrons with the total angular momentum $j = 5/2$. In these models, we have introduced effective interactions between f electrons to realize the Γ_3 CEF state as the ground state of an f^2 ion. First, we have derived the multipole interactions in the strong coupling limit^{33,34}. Then, we have found that two-orbital models are insufficient to discuss multipole physics of the Γ_3 systems. On the other hand, the derived multipole interactions for a three-orbital model depend reasonably on lattice structure.

We have also investigated superconductivity in the Γ_3 system by applying a random phase approximation (RPA) to the three-orbital model^{35,36}. Then, we have found instability to the E_g spin-singlet superconductivity. Such d -wave superconductivity is naturally expected in this model by the following reason. We have introduced an antiferromagnetic interaction between the orbitals belonging to Γ_7 and Γ_8 symmetry to stabilize the f^2 - Γ_3 CEF state. This interaction also works as an on-site spin-singlet pairing interaction between electrons in these orbitals. The orbital symmetry can be rewritten as $\Gamma_7 = \Gamma_2 \times \Gamma_6$ and $\Gamma_8 = \Gamma_3 \times \Gamma_6$, where Γ_6 describes the Kramers or spin degeneracy. Thus, the interorbital spin-singlet pairing state composed of the Γ_7 and Γ_8 orbitals on the same site has the E_g ($= \Gamma_3 = \Gamma_2 \times \Gamma_3$) symmetry. Such anisotropic superconductivity originating from

the orbital anisotropy was already discussed for a simple two-orbital Hubbard model³⁷.

When anisotropic superconductivity occurs in a cubic system, the lattice symmetry lowers with some exceptions such as a $d_{x^2-y^2} + id_{3z^2-r^2}$ state⁷. In this sense, $d_{x^2-y^2}$ and $d_{3z^2-r^2}$ superconductivities may be called as nematic superconductivity as in $\text{Cu}_x\text{Bi}_2\text{Se}_2$ ³⁸⁻⁴¹ and $\text{Nb}_x\text{Bi}_2\text{Se}_2$ ⁴². In a system with the quadrupole degrees of freedom like the Γ_3 system, the FQ moment should be finite in the nematic superconducting state. Thus, we expect a coexistent state of the d -wave superconductivity and FQ order in the Γ_3 system³⁶. In addition, superconductivity in $\text{PrT}_2\text{X}_{20}$ occurs in the quadrupole ordered phases in most cases. Thus, the coexistence with quadrupole order is important to understand the superconductivity in the Γ_3 system.

However, superconductivity in the Γ_3 system has been explored theoretically only by RPA in the normal state and characteristics of the coexistent phase is not yet clarified. Thus, theoretical studies for the ordered phase are highly desired. In addition to the coexistent phase, superconducting phase without quadrupole order is also interesting. The E_g superconducting state is degenerate and the time reversal breaking superconductivity of $d + id$ is possible as is discussed for URu_2Si_2 ⁴³⁻⁴⁵, graphene⁴⁶⁻⁴⁸, and SrPtAs ⁴⁹. If the $d + id$ state realizes, the superconducting transition temperature T_{SC} can be increased under uniaxial stress⁷, as in a $p + ip$ state discussed for Sr_2RuO_2 ^{50,51}.

In this paper, we investigate the coexistent state of the d -wave superconductivity and quadrupole order in the Γ_3 system by applying a mean-field theory to the three orbital model. In Sec. II, we introduce the mean-field Hamiltonian. In Sec. III, we show the calculated results for the coexistence phases of the superconductivity and quadrupole order. We also consider effects of uniaxial stress by introducing an external field to the quadrupole moment in Sec. IV. We summarize the paper in Sec. V

II. MEAN-FIELD HAMILTONIAN

A. Basis states and kinetic energy term

In this study, we consider the f -electron states with the total angular momentum $j = 5/2$ as the one-electron states. The $j = 7/2$ states have higher energy due to the spin-orbit interaction and we simply ignore them. The $j = 5/2$ states split into the Γ_7 and Γ_8 levels under a cubic CEF. The Γ_8 states at site \mathbf{r} are given by

$$c_{\mathbf{r}\alpha\uparrow}^*|0\rangle = \frac{1}{\sqrt{6}}(\sqrt{5}a_{\mathbf{r}5/2}^* + a_{\mathbf{r}-3/2}^*)|0\rangle, \quad (1)$$

$$c_{\mathbf{r}\alpha\downarrow}^*|0\rangle = \frac{1}{\sqrt{6}}(\sqrt{5}a_{\mathbf{r}-5/2}^* + a_{\mathbf{r}3/2}^*)|0\rangle, \quad (2)$$

$$c_{\mathbf{r}\beta\uparrow}^*|0\rangle = a_{\mathbf{r}1/2}^*|0\rangle, \quad (3)$$

$$c_{\mathbf{r}\beta\downarrow}^*|0\rangle = a_{\mathbf{r}-1/2}^*|0\rangle, \quad (4)$$

where $a_{\mathbf{r}j_z}^*$ is the creation operator of the electron with the z -component j_z of the total momentum at site \mathbf{r} and $|0\rangle$ denotes the vacuum state. We will use \dagger to denote the Hermitian conjugate of a matrix, and here, we have used $*$ to represent the creation operators to avoid confusion. The Γ_7 states are given by

$$c_{\mathbf{r}\gamma\uparrow}^*|0\rangle = \frac{1}{\sqrt{6}}(a_{\mathbf{r}5/2}^* - \sqrt{5}a_{\mathbf{r}-3/2}^*)|0\rangle, \quad (5)$$

$$c_{\mathbf{r}\gamma\downarrow}^*|0\rangle = \frac{1}{\sqrt{6}}(a_{\mathbf{r}-5/2}^* - \sqrt{5}a_{\mathbf{r}3/2}^*)|0\rangle. \quad (6)$$

In these states, $\sigma = \uparrow$ or \downarrow denotes the Kramers degeneracy of the one-electron states. While it is not a real spin due to the spin-orbit coupling, we call it spin for simplicity in the following.

In general, the conduction bands near the Fermi level are composed not only of the f orbital. However, in the present study, we consider an f -orbital only model as one of the simplest models to describe the Γ_3 systems. The influence of the other orbitals may be partially included in the effective f -electron hopping⁵². We consider the f -electron hopping through σ bonding ($ff\sigma$) on a simple cubic lattice^{53,54}. Then, the kinetic energy term is given by

$$H_{\text{kin}} = \sum_{\mathbf{k}\tau\tau'\sigma} c_{\mathbf{k}\tau\sigma}^* \xi_{\mathbf{k}\tau\tau'} c_{\mathbf{k}\tau'\sigma}, \quad (7)$$

with

$$\xi_{\mathbf{k}} = \begin{pmatrix} 3t(c_x + c_y) & -\sqrt{3}t(c_x - c_y) & 0 \\ -\sqrt{3}t(c_x - c_y) & t(c_x + c_y + 4c_z) & 0 \\ 0 & 0 & 0 \end{pmatrix}, \quad (8)$$

where $c_i = \cos k_i$ ($i = x, y, \text{ or } z$), $t = 3(ff\sigma)/14$, and we have set the lattice constant as unity. The bandwidth is $W = 12t$.

B. Mean-field Hamiltonian for quadrupole ordering

A one-electron operator and its Fourier transformation are written as

$$\hat{A}(\mathbf{r}) = \sum_{\tau\tau'\sigma} \tilde{A}_{\tau\tau'} c_{\mathbf{r}\tau\sigma}^* c_{\mathbf{r}\tau'\sigma}, \quad (9)$$

$$\begin{aligned} \hat{A}(\mathbf{q}) &= \frac{1}{N} \sum_{\mathbf{r}} e^{-i\mathbf{q}\cdot\mathbf{r}} \hat{A}(\mathbf{r}) \\ &= \frac{1}{N} \sum_{\tau\tau'\sigma\mathbf{k}} \tilde{A}_{\tau\tau'} c_{\mathbf{k}\tau\sigma}^* c_{\mathbf{k}+\mathbf{q}\tau'\sigma}, \end{aligned} \quad (10)$$

respectively. N is the number of the lattice sites. In the Γ_3 CEF state, the quadrupole moments of Γ_3 symmetry are active. The matrices for the Γ_3 quadrupole moments

are given by

$$\tilde{O}_2^0 = \frac{1}{\sqrt{42}} \begin{pmatrix} 4 & & \sqrt{5} \\ & -4 & \\ \sqrt{5} & & \end{pmatrix}, \quad (11)$$

$$\tilde{O}_2^2 = \frac{1}{\sqrt{42}} \begin{pmatrix} & 4 & \\ 4 & & -\sqrt{5} \\ & -\sqrt{5} & \end{pmatrix}, \quad (12)$$

where we have normalized them so as to satisfy $\text{Tr}(\tilde{O}_2^0)^2 = \text{Tr}(\tilde{O}_2^2)^2 = 1$. Here, Tr denotes the trace of a matrix. The intersite quadrupole interaction is given by

$$\begin{aligned} H_1^{(Q)} &= \sum_{AB(\mathbf{r}, \mathbf{r}')} J_{AB}(\mathbf{r} - \mathbf{r}') \hat{A}(\mathbf{r}) \hat{B}(\mathbf{r}') \\ &= \frac{N}{2} \sum_{AB\mathbf{q}} J_{AB}(\mathbf{q}) \hat{A}(-\mathbf{q}) \hat{B}(\mathbf{q}), \end{aligned} \quad (13)$$

where $(\mathbf{r}, \mathbf{r}')$ denotes a pair of lattice sites and

$$J_{AB}(\mathbf{q}) = \sum_{\mathbf{r}} e^{-i\mathbf{q}\cdot\mathbf{r}} J_{AB}(\mathbf{r}). \quad (14)$$

To deal with the effect of a uniaxial stress, we consider an external field to the quadrupole moments:

$$H_{\text{ext}}^{(Q)} = - \sum_{A\mathbf{r}} H_A(\mathbf{r}) \hat{A}(\mathbf{r}) = -N \sum_{A\mathbf{q}} H_A(-\mathbf{q}) \hat{A}(\mathbf{q}), \quad (15)$$

where

$$H_A(\mathbf{q}) = \frac{1}{N} \sum_{\mathbf{r}} e^{-i\mathbf{q}\cdot\mathbf{r}} H_A(\mathbf{r}). \quad (16)$$

For a uniaxial stress along the z direction, we vary $H_{20} \equiv H_{O_2^0}(\mathbf{q} = \mathbf{0})$.

We apply a mean-field approximation to the quadrupole interaction:

$$\begin{aligned} &H_1^{(Q)} + H_{\text{ext}}^{(Q)} \\ &\simeq \frac{N}{2} \sum_{AB\mathbf{q}} J_{AB}(\mathbf{q}) \left(\hat{A}(-\mathbf{q}) \langle \hat{B}(\mathbf{q}) \rangle + \langle \hat{A}(-\mathbf{q}) \rangle \hat{B}(\mathbf{q}) \right. \\ &\quad \left. - \langle \hat{A}(-\mathbf{q}) \rangle \langle \hat{B}(\mathbf{q}) \rangle \right) + H_{\text{ext}}^{(Q)} \\ &= \sum_{\mathbf{q}\sigma\mathbf{k}} c_{\mathbf{k}\sigma}^\dagger \Delta_{\mathbf{q}}^Q c_{\mathbf{k}+\mathbf{q}\sigma} + E_0^{(Q, I)} \\ &= H_1^{(\text{MF}, Q)} + E_0^{(Q, I)}. \end{aligned} \quad (17)$$

Here, we have introduced the following notations:

$$c_{\mathbf{k}\sigma} = \begin{pmatrix} c_{\mathbf{k}\alpha\sigma} \\ c_{\mathbf{k}\beta\sigma} \\ c_{\mathbf{k}\gamma\sigma} \end{pmatrix}, \quad (18)$$

$$\Delta_{\mathbf{q}}^Q = \sum_B \left[\sum_A J_{AB}(\mathbf{q}) \langle \hat{A}(-\mathbf{q}) \rangle - H_B(-\mathbf{q}) \right] \tilde{B}, \quad (19)$$

$$E_0^{(Q, I)} = -\frac{N}{2} \sum_{AB\mathbf{q}} J_{AB}(\mathbf{q}) \langle \hat{A}(-\mathbf{q}) \rangle \langle \hat{B}(\mathbf{q}) \rangle. \quad (20)$$

$\langle \dots \rangle$ denotes the expectation value. In the following, we denotes the expectation value also as $A(\mathbf{q}) = \langle \hat{A}(\mathbf{q}) \rangle$. In this study, we consider ordering with $\mathbf{q} = \mathbf{0}$ and $\mathbf{q} = \mathbf{Q} = (\pi, \pi, \pi)$. Then, the mean-field Hamiltonian is written as

$$\begin{aligned} &H^{(\text{MF}, Q)} \\ &= H_{\text{kin}} + H_1^{(\text{MF}, Q)} \\ &= \sum_{\sigma\mathbf{k} \in \text{FBZ}} (c_{\mathbf{k}\sigma}^\dagger c_{\mathbf{k}+\mathbf{Q}\sigma}^\dagger) \begin{pmatrix} \xi_{\mathbf{k}} + \Delta_{\mathbf{0}}^Q & \Delta_{\mathbf{Q}}^Q \\ \Delta_{\mathbf{Q}}^Q & \xi_{\mathbf{k}+\mathbf{Q}} + \Delta_{\mathbf{0}}^Q \end{pmatrix} \begin{pmatrix} c_{\mathbf{k}\sigma} \\ c_{\mathbf{k}+\mathbf{Q}\sigma} \end{pmatrix} \\ &= \sum_{\sigma\mathbf{k} \in \text{FBZ}} c_{\sigma}^\dagger(\mathbf{k}) \xi(\mathbf{k}) c_{\sigma}(\mathbf{k}). \end{aligned} \quad (21)$$

The \mathbf{k} summation runs over the folded Brillouin-zone (FBZ) of the staggered ordering with \mathbf{Q} .

We also consider onsite Coulomb interactions: intra-orbital Coulomb interactions U_7 for the Γ_7 orbital and U_8 for the Γ_8 orbitals and interorbital Coulomb interaction U_8' for the Γ_8 orbitals. These interactions are also included within the mean-field approximation. For this purpose, we define charge operators by the following matrices:

$$\tilde{n}_\alpha = \begin{pmatrix} 1 & & \\ & 0 & \\ & & 0 \end{pmatrix}, \tilde{n}_\beta = \begin{pmatrix} 0 & & \\ & 1 & \\ & & 0 \end{pmatrix}, \tilde{n}_\gamma = \begin{pmatrix} 0 & & \\ & 0 & \\ & & 1 \end{pmatrix}. \quad (22)$$

The mean fields from the Coulomb interactions are written as the mean fields for charge interactions with $J_{n_\alpha n_\alpha}(\mathbf{q}) = J_{n_\beta n_\beta}(\mathbf{q}) = U_8/2$, $J_{n_\gamma n_\gamma}(\mathbf{q}) = U_7/2$, and $J_{n_\alpha n_\beta}(\mathbf{q}) = J_{n_\beta n_\alpha}(\mathbf{q}) = U_8'$. Then, the effects of the Coulomb interactions can be included in the above formulation for the quadrupole interaction. Without the Coulomb interactions, we find a tendency toward phase separation in particular for a strong quadrupole interaction. Since the phase separation is not our concern in this study, we have introduced the Coulomb interactions to alleviate this tendency.

In actual calculations, we consider ordering states with the principal axis along the z direction. Then, we assume interactions purely for O_2^0 or O_2^2 . We denote them as $J_{O_2^0 O_2^0}(\mathbf{q}) = J_{20}(\mathbf{q})$ and $J_{O_2^2 O_2^2}(\mathbf{q}) = J_{22}(\mathbf{q})$.

C. Mean-field Hamiltonian for superconductivity

For superconductivity, we assume the following interaction for spin-singlet pairing:

$$\begin{aligned}
H_1^{(\text{SC})} &= -\frac{1}{N} \sum_{\tau\tau'\mathbf{k}\mathbf{k}'\mathbf{q}} \frac{V_{\tau\tau'}(\mathbf{q})}{4} \\
&\quad \times (c_{-\mathbf{k}\tau\downarrow}^* c_{\mathbf{k}+\mathbf{q}\tau'\uparrow}^* - c_{-\mathbf{k}\tau\uparrow}^* c_{\mathbf{k}+\mathbf{q}\tau'\downarrow}^*) \\
&\quad \times (c_{\mathbf{k}'+\mathbf{q}\tau\uparrow} c_{-\mathbf{k}'\tau'\downarrow} - c_{\mathbf{k}'+\mathbf{q}\tau\downarrow} c_{-\mathbf{k}'\tau'\uparrow}) \\
&\simeq -\frac{1}{N} \sum_{\tau\tau'\mathbf{k}\mathbf{k}'\mathbf{q}} \frac{V_{\tau\tau'}(\mathbf{q})}{4} \\
&\quad \times \left[(c_{-\mathbf{k}\tau\downarrow}^* c_{\mathbf{k}+\mathbf{q}\tau'\uparrow}^* - c_{-\mathbf{k}\tau\uparrow}^* c_{\mathbf{k}+\mathbf{q}\tau'\downarrow}^*) \right. \\
&\quad \times \langle c_{\mathbf{k}'+\mathbf{q}\tau\uparrow} c_{-\mathbf{k}'\tau'\downarrow} - c_{\mathbf{k}'+\mathbf{q}\tau\downarrow} c_{-\mathbf{k}'\tau'\uparrow} \rangle \\
&\quad + \langle c_{-\mathbf{k}\tau\downarrow}^* c_{\mathbf{k}+\mathbf{q}\tau'\uparrow}^* - c_{-\mathbf{k}\tau\uparrow}^* c_{\mathbf{k}+\mathbf{q}\tau'\downarrow}^* \rangle \\
&\quad \times (c_{\mathbf{k}'+\mathbf{q}\tau\uparrow} c_{-\mathbf{k}'\tau'\downarrow} - c_{\mathbf{k}'+\mathbf{q}\tau\downarrow} c_{-\mathbf{k}'\tau'\uparrow}) \\
&\quad \left. - \langle c_{-\mathbf{k}\tau\downarrow}^* c_{\mathbf{k}+\mathbf{q}\tau'\uparrow}^* - c_{-\mathbf{k}\tau\uparrow}^* c_{\mathbf{k}+\mathbf{q}\tau'\downarrow}^* \rangle \right] \\
&\quad \times \langle c_{\mathbf{k}'+\mathbf{q}\tau\uparrow} c_{-\mathbf{k}'\tau'\downarrow} - c_{\mathbf{k}'+\mathbf{q}\tau\downarrow} c_{-\mathbf{k}'\tau'\uparrow} \rangle.
\end{aligned} \tag{23}$$

The superconducting pairing interaction is symmetric with respect to the orbital index: $V_{\tau\tau'}(\mathbf{q}) = V_{\tau'\tau}(\mathbf{q})$. While we will consider only pairing states with total momentum $\mathbf{q} = \mathbf{0}$ in actual calculation, here we write down equations keeping both pairing states with $\mathbf{q} = \mathbf{0}$ and \mathbf{Q} . Then, the superconducting pairing interaction term is approximated as

$$\begin{aligned}
H_1^{(\text{SC})} &\simeq \sum_{\mathbf{k} \in \text{FBZ}} \left[c_{\uparrow}^{\dagger}(\mathbf{k}) \Delta c_{\downarrow}^*(-\mathbf{k}) + c_{\downarrow}^{\dagger}(-\mathbf{k}) \Delta^{\dagger} c_{\uparrow}(\mathbf{k}) \right] \\
&\quad + E_0^{(\text{SC}, \text{I})},
\end{aligned} \tag{24}$$

where T denotes the transpose of a matrix,

$$\Delta = \begin{pmatrix} \Delta_0^{\text{SC}} & \Delta_{\mathbf{Q}}^{\text{SC}} \\ \Delta_{\mathbf{Q}}^{\text{SC}} & \Delta_0^{\text{SC}} \end{pmatrix}, \tag{25}$$

$$\Delta_{\mathbf{q}\tau\tau'}^{\text{SC}} = \frac{V_{\tau\tau'}(\mathbf{q})}{N} \sum_{\mathbf{k}} \frac{1}{2} \langle c_{\mathbf{k}+\mathbf{q}\tau\uparrow} c_{-\mathbf{k}\tau'\downarrow} - c_{\mathbf{k}+\mathbf{q}\tau\downarrow} c_{-\mathbf{k}\tau'\uparrow} \rangle, \tag{26}$$

and

$$E_0^{(\text{SC}, \text{I})} = N \sum_{\mathbf{q}\tau\tau', V_{\tau\tau'}(\mathbf{q}) \neq 0} |\Delta_{\tau\tau'\mathbf{q}}^{\text{SC}}|^2 / V_{\tau\tau'}(\mathbf{q}). \tag{27}$$

We call the quantity without the factor $V_{\tau\tau'}(\mathbf{q})$ in Eq. (26) the pair amplitude.

The total Hamiltonian is approximated as

$$\begin{aligned}
H &= H_{\text{kin}} + H_1^{(\text{Q})} + H_{\text{ext}}^{(\text{Q})} + H_1^{(\text{SC})} \\
&\simeq H^{(\text{MF})} + \sum_{\mathbf{k} \in \text{FBZ}} \text{Tr} \xi(\mathbf{k}) + E_0^{(\text{Q}, \text{I})} + E_0^{(\text{SC}, \text{I})} \\
&= H^{(\text{MF})} + E_0,
\end{aligned} \tag{28}$$

where the mean-field Hamiltonian is given by

$$\begin{aligned}
H^{(\text{MF})} &= \sum_{\mathbf{k} \in \text{FBZ}} (c_{\uparrow}^{\dagger}(\mathbf{k}) \ c_{\downarrow}^{\dagger}(-\mathbf{k})) \begin{pmatrix} \xi(\mathbf{k}) & \Delta \\ \Delta^{\dagger} & -\xi^{\text{T}}(-\mathbf{k}) \end{pmatrix} \begin{pmatrix} c_{\uparrow}(\mathbf{k}) \\ c_{\downarrow}^*(-\mathbf{k}) \end{pmatrix}.
\end{aligned} \tag{29}$$

We solve the mean-field Hamiltonian self-consistently. When we obtain different solutions, we select the state with the lowest free-energy. For the evaluation of the free-energy, we need to calculate the constant term E_0 in Eq. (28).

In previous studies³³⁻³⁶, we have considered an antiferromagnetic interaction $H_J = J \sum_{\mathbf{r}} \mathbf{s}_{\mathbf{r}7} \cdot \mathbf{s}_{\mathbf{r}8}$ between electrons in the Γ_7 and Γ_8 orbitals to realize the Γ_3 state as the ground state of an f^2 ion, where $\mathbf{s}_{\mathbf{r}7} = (1/2) \sum_{\sigma\sigma'} c_{\mathbf{r}\gamma\sigma}^{\dagger} \boldsymbol{\sigma}_{\sigma\sigma'} c_{\mathbf{r}\gamma\sigma'}$ and $\mathbf{s}_{\mathbf{r}8} = (1/2) \sum_{\sigma\sigma'\nu=\alpha,\beta} c_{\mathbf{r}\nu\sigma}^{\dagger} \boldsymbol{\sigma}_{\sigma\sigma'} c_{\mathbf{r}\nu\sigma'}$. $\boldsymbol{\sigma}$ are the Pauli matrices. This interaction results in \mathbf{q} -independent pairing interactions $V_{\alpha\gamma}(\mathbf{q}) = V_{\beta\gamma}(\mathbf{q}) = 3J/4$. However, in this study, we consider ordinary pairing states with total momentum $\mathbf{q} = \mathbf{0}$, and then, we include only $V_{\alpha\gamma}(\mathbf{0})$ and $V_{\beta\gamma}(\mathbf{0})$ for simplicity. We change these pairing interactions independently to investigate the relation between the quadrupole ordering and superconducting symmetry.

The superconducting order parameter $\Delta_{\alpha\gamma}^{\text{SC}}$ transforms as $k_x^2 - k_y^2$ under symmetry operations. We consider this $d_{x^2-y^2}$ superconducting pairing state and denote $\Delta_{\alpha\gamma}^{\text{SC}} = \Delta_{x^2-y^2}$ and $V_{\alpha\gamma}(\mathbf{0}) = V_{x^2-y^2}$. Similarly, we consider the $d_{3z^2-r^2}$ superconducting pairing state with $\Delta_{\beta\gamma}^{\text{SC}} \neq 0$ and denote $\Delta_{\beta\gamma}^{\text{SC}} = \Delta_{3z^2-r^2}$ and $V_{\beta\gamma}(\mathbf{0}) = V_{3z^2-r^2}$.

III. QUADRUPOLE ORDER AND SUPERCONDUCTIVITY

In the following calculations, we set $U_7 = 5t$, $U_8 = 10t$, and $U_8' = 5t$. We vary $V_{x^2-y^2}$, $V_{3z^2-r^2}$, $J_{20}(\mathbf{q})$, and $J_{20}(\mathbf{q})$ with $\mathbf{q} = \mathbf{0}$ and \mathbf{Q} , but they are set to zero unless finite values are explicitly given. To realize the Γ_3 state as the CEF ground state of an f^2 ion, the following conditions should be satisfied³³: $n_7 = \sum_{\sigma} \langle c_{\mathbf{k}\gamma\sigma}^* c_{\mathbf{k}\gamma\sigma} \rangle / N \simeq 1$ and $n_8 = \sum_{\sigma,\tau=\alpha,\beta} \langle c_{\mathbf{k}\tau\sigma}^* c_{\mathbf{k}\tau\sigma} \rangle / N \simeq 1$. We tune the chemical potential for each CEF level independently so as to satisfy the conditions $n_7 = 1$ and $n_8 = 1$. The lattice size is $N = L \times L \times L$ with $L = 12$. We have found that the finite size effect is weak. In evaluating transition temperatures, we extrapolate the order parameters to zero by using data with temperature intervals of $dT = 0.02t$. The differences in the transition temperatures obtained with $L = 8$ and $L = 12$ are smaller than the errors in this extrapolation.

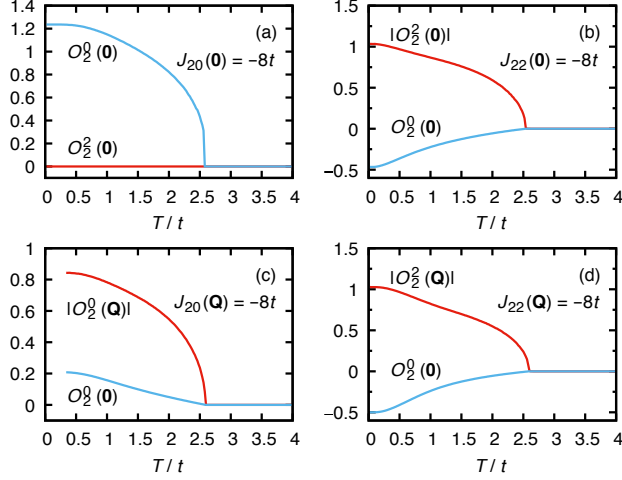


FIG. 1. Temperature dependence of the quadrupole order parameters (a) for $J_{20}(\mathbf{0}) = -8t$, (b) for $J_{22}(\mathbf{0}) = -8t$, (c) for $J_{20}(\mathbf{Q}) = -8t$, and (d) for $J_{22}(\mathbf{Q}) = -8t$.

A. Temperature dependence of order parameters

First, we show the temperature dependence of the quadrupole moment without superconducting interactions. In an ordered state of O_2^0 or O_2^2 with any periodicity, the z direction becomes inequivalent to the x and y directions and the FQ moment $O_2^0(\mathbf{0})$ should be induced³⁶. In particular, $O_2^0(\mathbf{0})$ is induced by the FQ order of O_2^0 itself, and as a result, the transition becomes of first order. This is also understood from the existence of the third-order term in the Landau free-energy^{55,56}. Due to the self-induced nature of the $O_2^0(\mathbf{0})$ order, the transition temperature of $O_2^0(\mathbf{0})$ is higher than that of $O_2^2(\mathbf{0})$ as long as $J_{20}(\mathbf{0}) = J_{22}(\mathbf{0})$, under which the cubic symmetry of the interaction term is retained⁵⁷. Indeed, the order parameter of the FQ order in $\text{PrTi}_2\text{Al}_{20}$ is determined to be O_2^0 ^{20,31}. However, in the following, we change $J_{20}(\mathbf{0})$ and $J_{22}(\mathbf{0})$ independently to clarify the relation between superconductivity and kinds of the quadrupole order.

In Fig. 1(a), we show temperature dependence of $O_2^0(\mathbf{0})$ for $J_{20}(\mathbf{0}) = -8t$. As discussed above, the transition is of first order and $O_2^0(\mathbf{0})$ jumps at the transition temperature. For comparison, we also show $O_2^2(\mathbf{0})$ but it remains zero. Note that the solutions with positive and negative O_2^0 are not equivalent. In the present model, we find that the solution with positive O_2^0 has lower free-energy. In Fig. 1(b), we show temperature dependence of the order parameter $O_2^2(\mathbf{0})$ for $J_{22}(\mathbf{0}) = -8t$. The transition temperature is slightly lower than that in Fig. 1(a). As discussed above, $O_2^0(\mathbf{0})$ is induced below the transition temperature. The induced $O_2^0(\mathbf{0})$ is negative. As for AFQ ordering cases, we show results for $J_{20}(\mathbf{Q}) = -8t$ and for $J_{22}(\mathbf{Q}) = -8t$ in Fig. 1(c) and (d), respectively. The induced moment $O_2^0(\mathbf{0})$ has the opposite sign between these two cases.

Next, we show the temperature dependence of the su-

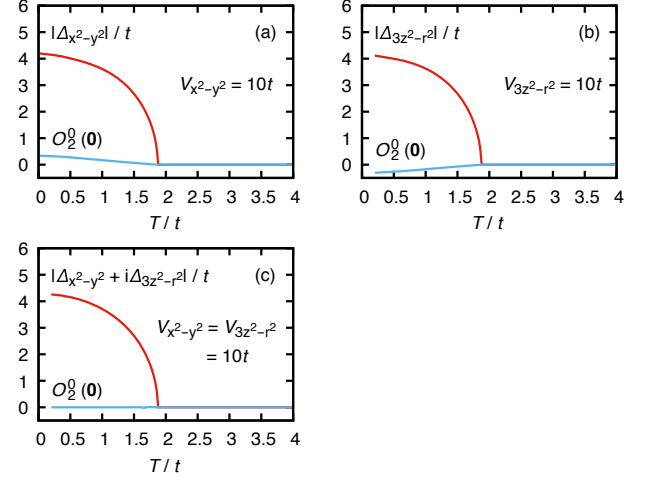


FIG. 2. Temperature dependence of the superconducting order parameters (a) for $V_{x^2-y^2} = 10t$, (b) for $V_{3z^2-r^2} = 10t$, and (c) for $V_{x^2-y^2} = V_{3z^2-r^2} = 10t$. The induced $O_2^0(\mathbf{0})$ is also shown.

perconducting order parameters without quadrupole interactions. Although we should set $V_{x^2-y^2} = V_{3z^2-r^2}$ to retain the cubic symmetry in the interaction term, we change them independently to understand the relation between superconducting symmetry and quadrupole order. Figure 2(a) shows temperature dependence of $\Delta_{x^2-y^2}$ for $V_{x^2-y^2} = 10t$. Below the transition temperature, positive $O_2^0(\mathbf{0})$ is induced. For $V_{3z^2-r^2} = 10t$ [Fig. 2(b)], $d_{3z^2-r^2}$ superconductivity occurs at the same transition temperature as in Fig. 2(a). The induced $O_2^0(\mathbf{0})$ has the opposite sign between the $d_{x^2-y^2}$ and $d_{3z^2-r^2}$ superconducting states. We can understand this from the Ginzburg–Landau theory. At least around the transition temperature, i.e., when the order parameters are sufficiently small, the coupling constant of the superconducting order parameter to $O_2^0(\mathbf{0})$ in the Ginzburg–Landau free-energy has the opposite sign between the $d_{x^2-y^2}$ and $d_{3z^2-r^2}$ superconducting states⁷.

Note also that the $d_{3z^2-r^2}$ superconducting state accompanying the FQ order of O_2^0 mixes with s -wave superconductivity since $3z^2 - r^2$ is an identity representation in the tetragonal phase. When we consider the s -wave superconducting interaction and if the FQ moment of O_2^0 develops sufficiently, the effect of the hybridization between these superconducting states may become strong. For example, line nodes in the gap function in the $d_{3z^2-r^2}$ superconductivity can disappear at lower temperatures due to this hybridization.

For $V_{x^2-y^2} = V_{3z^2-r^2}$, according to the Ginzburg–Landau theory⁷, superconducting symmetry is $d_{x^2-y^2}$, $d_{3z^2-r^2}$, or $d_{x^2-y^2} + id_{3z^2-r^2}$ depending on the microscopic model. In the present model, we find $d_{x^2-y^2} + id_{3z^2-r^2}$ superconductivity as shown in Fig. 2(c). In this superconducting state, the cubic symmetry is preserved, since $d_{x^2-y^2} + id_{3z^2-r^2} = e^{-2\pi i/3}(d_{y^2-z^2} + id_{3x^2-r^2}) = e^{2\pi i/3}(d_{z^2-x^2} + id_{3y^2-r^2})$. Then, the quadrupole moment

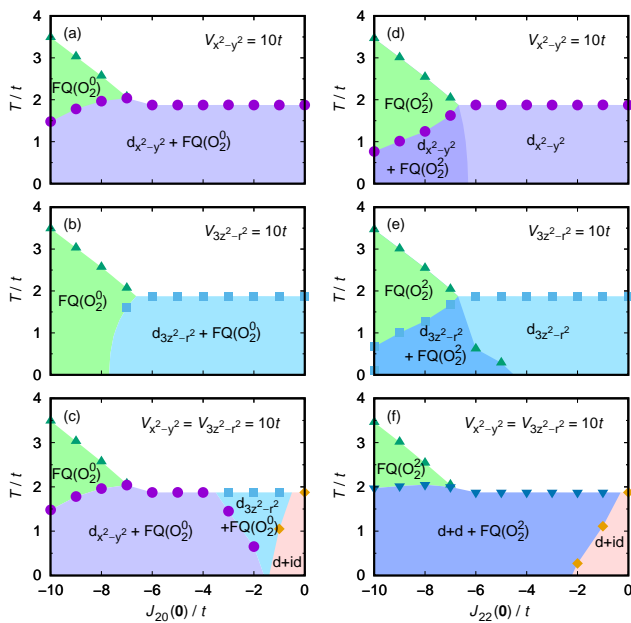


FIG. 3. Phase diagrams of superconductivity coexisting with FQ order: in the $J_{20}(\mathbf{0})$ - T plane (a) for $V_{x^2-y^2} = 10t$, (b) for $V_{3z^2-r^2} = 10t$, and (c) for $V_{x^2-y^2} = V_{3z^2-r^2} = 10t$; in the $J_{22}(\mathbf{0})$ - T plane (d) for $V_{x^2-y^2} = 10t$, (e) for $V_{3z^2-r^2} = 10t$, and (f) for $V_{x^2-y^2} = V_{3z^2-r^2} = 10t$.

$O_2^0(\mathbf{0})$ is not induced in this case. In the $d+id$ superconducting state, the superconducting gap has only point nodes at $|k_x| = |k_y| = |k_z|$ while line nodes appear in the $d_{x^2-y^2}$ and $d_{3z^2-r^2}$ superconducting states. It may be natural that the superconductivity with a larger gapped portion of the Fermi surface is more stable at least without quadrupole interactions.

B. Phase diagrams

In this subsection, we construct phase diagrams by changing the strength of the quadrupole interaction and temperature with fixing the values of the superconducting pairing interactions. In the following, while we do not explicitly denote, all the ordered phases accompany a FQ moment of O_2^0 except for the pure $d+id$ superconducting phase.

In Fig. 3(a) and (b), we show phase diagrams in the $J_{20}(\mathbf{0})$ - T plane for $V_{x^2-y^2} = 10t$ and for $V_{3z^2-r^2} = 10t$, respectively. The region of the $d_{x^2-y^2}$ superconducting phase in Fig. 3(a) is wider than that of the $d_{3z^2-r^2}$ superconducting phase in Fig. 3(b). As shown in Fig. 1(a) and Fig. 2(a), both the pure FQ order of O_2^0 and the $d_{x^2-y^2}$ superconducting state accompany positive $O_2^0(\mathbf{0})$ in the present model and they are expected to be cooperative. Indeed, the superconducting transition temperature around $J_{20}(\mathbf{0}) = -7t$ is higher than that without the quadrupole interaction, while a too large $|J_{20}(\mathbf{0})|$ suppresses T_{SC} . On the other hand, the $d_{3z^2-r^2}$ super-

conducting state induces negative $O_2^0(\mathbf{0})$ and the FQ order of O_2^0 is destructive for this superconducting state as shown in Fig. 3(b). For $V_{x^2-y^2} = V_{3z^2-r^2} = 10t$ shown in Fig. 3(c), the $d+id$ state appears for a small $|J_{20}(\mathbf{0})|$. The $d_{x^2-y^2}$ state appears for larger $|J_{20}(\mathbf{0})|$ in a wide range since this superconducting state is cooperative with the FQ order of O_2^0 . The $d_{3z^2-r^2}$ state appears in a narrow region between the above two superconducting phases. In each of the phase diagrams Fig. 3(a) and (b), only one superconducting phase appears since the FQ moment of O_2^0 is always finite even without the FQ interaction. This is in sharp contrast to the other quadrupole interaction cases we will discuss below.

In PrTi₂Al₂₀ under hydrostatic pressure^{29,30}, T_{SC} seems to have a peak at around pressure where T_{SC} reaches T_{FQ} of O_2^0 . The phase diagram Fig. 3(a) or (c) may be relevant to PrTi₂Al₂₀ if a hydrostatic pressure mainly affects the intersite quadrupole interactions. This is a natural assumption when the superconducting pair is mainly composed of the same site³⁵ and insensitive to the change in the distance between lattice sites.

In Fig. 3(d) and (e), we show phase diagrams in the $J_{22}(\mathbf{0})$ - T plane for $V_{x^2-y^2} = 10t$ and for $V_{3z^2-r^2} = 10t$, respectively. For $V_{3z^2-r^2} = 10t$ at $J_{22}(\mathbf{0}) = -10t$, superconductivity disappears at a very low temperature. There are two superconducting phases with and without FQ order of O_2^0 in each phase diagram. The region of the coexisting phase of the $d_{3z^2-r^2}$ superconductivity with FQ order of O_2^0 seems slightly larger than that of the $d_{x^2-y^2}$ superconductivity. It may be understood from the fact that the induced $O_2^0(\mathbf{0})$ in the $d_{3z^2-r^2}$ superconductivity and FQ order of O_2^0 has the same sign. In the FQ ordered phase of O_2^0 , the symmetry is lower than tetragonal, i.e., orthorhombic. Then, in the coexisting phase of the superconductivity and the FQ order of O_2^0 , both the pair amplitudes for $d_{x^2-y^2}$ and $d_{3z^2-r^2}$ become finite. Thus, for $V_{x^2-y^2} = V_{3z^2-r^2} = 10t$ [Fig. 3(f)], by combining both superconducting order parameters, $d+d$ superconducting phase realizes in a wide region.

For O_2^0 AFQ ordering cases, we obtain similar phase diagrams for $V_{x^2-y^2} = 10t$ and for $V_{3z^2-r^2} = 10t$ except for the superconducting symmetry [Fig. 4(a) and (b)]. We suppose that the effect of the induced $O_2^0(\mathbf{0})$ in the AFQ order on superconductivity is weak. Indeed, for $V_{x^2-y^2} = V_{3z^2-r^2} = 10t$ [Fig. 4(c)], the $d+id$ state without $O_2^0(\mathbf{0})$ realizes in a wide region. Also for O_2^0 AFQ ordering cases, the effect of the induced $O_2^0(\mathbf{0})$ seems weak. We obtain similar phase diagrams for $V_{x^2-y^2} = 10t$ and for $V_{3z^2-r^2} = 10t$ [Fig. 4(d) and (e)], and the $d+id$ state realizes in a wide region for $V_{x^2-y^2} = V_{3z^2-r^2} = 10t$ [Fig. 4(f)]. In all of these AFQ order cases, there are superconducting phases with and without AFQ order.

In a coexisting state of superconductivity and staggered order with ordering vector \mathbf{Q} , the pair amplitude with momentum \mathbf{Q} can be finite. In the AFQ order of O_2^0 , a matrix element between (α, \mathbf{k}) and $(\alpha, \mathbf{k} + \mathbf{Q})$ becomes finite [see Eq. (11)]. Here, (τ, \mathbf{k}) denotes the electronic state of orbital τ with momentum \mathbf{k} . Then, if the

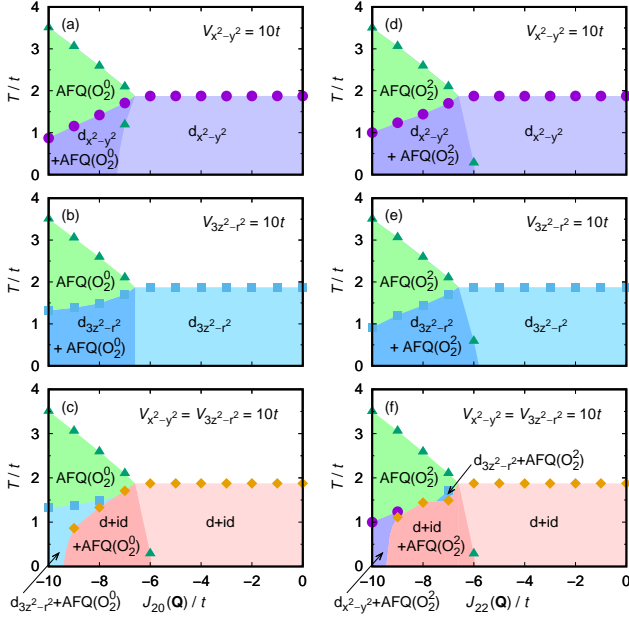


FIG. 4. Phase diagrams of superconductivity coexisting with AFQ order: in the $J_{20}(\mathbf{Q})$ - T plane (a) for $V_{x^2-y^2} = 10t$, (b) for $V_{3z^2-r^2} = 10t$, and (c) for $V_{x^2-y^2} = V_{3z^2-r^2} = 10t$: in the $J_{22}(\mathbf{Q})$ - T plane (d) for $V_{x^2-y^2} = 10t$, (e) for $V_{3z^2-r^2} = 10t$, and (f) for $V_{x^2-y^2} = V_{3z^2-r^2} = 10t$.

pair amplitude of (α, \mathbf{k}) and $(\gamma, -\mathbf{k})$ is finite, the pair amplitude of $(\alpha, \mathbf{k} + \mathbf{Q})$ and $(\gamma, -\mathbf{k})$ is also finite in the AFQ order of O_2^0 . In other words, the pair amplitude of $d_{x^2-y^2}$ with \mathbf{Q} is induced in the coexisting phase of the $d_{x^2-y^2}$ superconductivity with O_2^0 AFQ order. Similarly, the $d_{3z^2-r^2}$ superconductivity with AFQ order of O_2^0 accompanies the pair amplitude of $d_{3z^2-r^2}$ with \mathbf{Q} . In the AFQ order of O_2^0 , a matrix element between (α, \mathbf{k}) and $(\beta, \mathbf{k} + \mathbf{Q})$ becomes finite [see Eq. (12)]. Then, in the coexisting phase of the $d_{x^2-y^2}$ superconductivity and AFQ order of O_2^0 , the pair amplitude of $d_{3z^2-r^2}$ with momentum \mathbf{Q} becomes finite. For the $d_{3z^2-r^2}$ superconductivity with AFQ order of O_2^0 , the pair amplitude of $d_{x^2-y^2}$ with \mathbf{Q} is finite. In the coexisting phase of the $d+id$ superconductivity with O_2^0 or O_2^2 AFQ order, the pair amplitude for $d+id$ with \mathbf{Q} becomes finite. We have checked these induced pair amplitudes with momentum \mathbf{Q} in the coexisting phases of the superconductivity with AFQ order in the numerical calculations.

To show the dependence on the strength of the superconducting interaction, we have constructed a phase diagram of $d_{x^2-y^2}$ superconductivity coexisting with FQ order of O_2^0 for a smaller value of the superconducting interaction, $V_{x^2-y^2} = 5t$, as an example (Fig. 5). This phase diagram is qualitatively the same as for $V_{x^2-y^2} = 10t$ in Fig. 3(a). For example, we observe an enhancement of the superconducting transition temperature at a parameter where $T_{SC} \simeq T_{FQ}$. However, we find that the superconductivity disappears for a much smaller value of the superconducting interaction. Thus, we need a certain

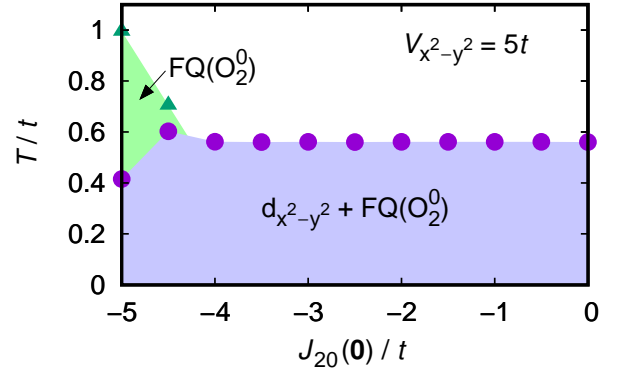


FIG. 5. Phase diagram of $d_{x^2-y^2}$ superconductivity coexisting with FQ order of O_2^0 for $V_{x^2-y^2} = 5t$.

strength of the superconducting interaction to discuss superconductivity in the present mean-field model.

IV. UNIAXIAL STRESS

To investigate the effect of uniaxial stress, we vary the external field H_{20} to the quadrupole moment O_2^0 . This field corresponds to a uniaxial stress along the z direction. From the definition in Eq. (15), positive H_{20} increases $O_2^0(\mathbf{0})$ and negative H_{20} decreases $O_2^0(\mathbf{0})$.

First, we consider FQ order of O_2^0 without superconductivity. In this case under $H_{20} \neq 0$, the FQ transition of O_2^0 is not a symmetry breaking transition since O_2^0 is already finite by H_{20} . Then, if the FQ transition exists, it should be of first order. Since the FQ moment is positive without H_{20} , $H_{20} < 0$ suppresses T_{FQ} . For $H_{20} > 0$, T_{FQ} can be enhanced; however, the FQ transition becomes a crossover at a small value of H_{20} since the discontinuity in the order parameter at the first order transition is small even at $H_{20} = 0$ [Fig. 1(a)].

For other pure order cases, the transition temperature increases under $H_{20} > 0$ ($H_{20} < 0$) at least for a sufficiently small $|H_{20}|$ when the induced $O_2^0(\mathbf{0})$ is positive (negative) at $H_{20} = 0$. The transition temperature increases under $H_{20} > 0$ for AFQ order of O_2^0 and for the superconductivity of $d_{x^2-y^2}$. The transition temperature increases under $H_{20} < 0$ for FQ of order O_2^2 , for AFQ order of O_2^2 , and for the superconductivity of $d_{3z^2-r^2}$. These behaviors seem rather trivial and we do not show phase diagrams for these cases here.

For the $d+id$ superconductivity, T_{SC} is expected to split into two by H_{20} ⁷. We demonstrate it in the present mean-field model. Figure 6 shows a phase diagram in the H_{20} - T plane for $V_{x^2-y^2} = V_{3z^2-r^2} = 10t$. The transition temperature is split into two by H_{20} . The higher transition temperature is slightly increased by H_{20} . Below the second superconducting transition temperature, $d+id$ superconducting state appears. The weights of the

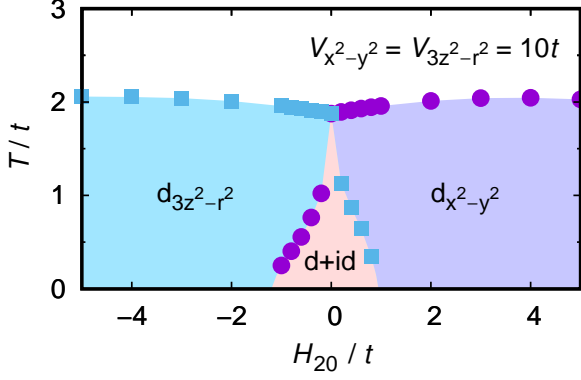


FIG. 6. Phase diagram of superconductivity in the H_{20} - T plane without quadrupole interactions for $V_{x^2-y^2} = V_{3z^2-r^2} = 10t$.

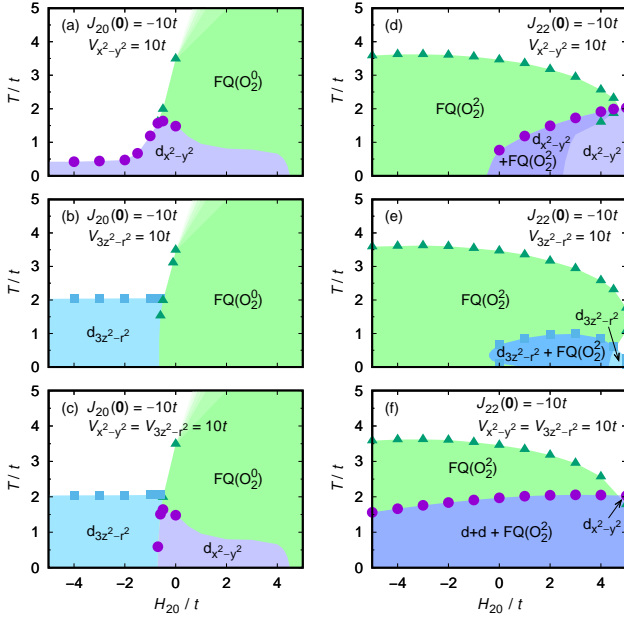


FIG. 7. Phase diagrams of superconductivity coexisting with FQ order in the H_{20} - T plane: with $J_{20}(\mathbf{0}) = -10t$ (a) for $V_{x^2-y^2} = 10t$, (b) for $V_{3z^2-r^2} = 10t$, and (c) for $V_{x^2-y^2} = V_{3z^2-r^2} = 10t$; with $J_{22}(\mathbf{0}) = -10t$ (d) for $V_{x^2-y^2} = 10t$, (e) for $V_{3z^2-r^2} = 10t$, and (f) for $V_{x^2-y^2} = V_{3z^2-r^2} = 10t$.

$d_{x^2-y^2}$ and $d_{3z^2-r^2}$ components in the $d + id$ superconducting state are different for $H_{20} \neq 0$. For a large $|H_{20}|$, only one superconducting transition occurs. The region of the $d + id$ superconductivity is narrow in the present model.

Next, we discuss the effects of the uniaxial stress on the coexisting phases of superconductivity with FQ order. Figure 7(a) is a phase diagram for $J_{20}(\mathbf{0}) = -10t$ and $V_{x^2-y^2} = 10t$. For $H_{20} \gtrsim 0$, the FQ transition of O_2^0 becomes a crossover. At low temperatures for $H_{20} \gtrsim 0$, we find a solution with the $d_{x^2-y^2}$ superconductivity

but it does not fulfill the condition $n_7 = n_8 = 1$. It implies that phase separation occurs. While the $d_{x^2-y^2}$ superconductivity may survive to some extent for $H_{20} > 0$, we should consider possible phase separation for this region. For $H_{20} < 0$, the FQ order of O_2^0 is suppressed and T_{SC} initially increases. By decreasing H_{20} further, both the FQ order of O_2^0 and $d_{x^2-y^2}$ superconductivity are suppressed as for the pure ordered phases of them. For $J_{20}(\mathbf{0}) = -10t$ and $V_{3z^2-r^2} = 10t$ [Fig. 7(b)], we find only the FQ phase of O_2^0 for $H_{20} > 0$ since a positive H_{20} suppresses the $d_{3z^2-r^2}$ superconductivity. On the other hand, for $H_{20} < 0$, the FQ order of O_2^0 is suppressed and the $d_{3z^2-r^2}$ superconductivity is realized in a wide region. For $J_{20}(\mathbf{0}) = -10t$ with $V_{x^2-y^2} = V_{3z^2-r^2} = 10t$ [Fig. 7(c)], we obtain a phase diagram like a combination of Fig. 7(a) and (b). Then, we expect a change of the superconducting symmetry by applying uniaxial stress for this case.

Figure 7(d) is a phase diagram for $J_{22}(\mathbf{0}) = -10t$ and $V_{x^2-y^2} = 10t$. For $H_{20} > 0$, the FQ order of O_2^2 is suppressed and $d_{x^2-y^2}$ superconductivity develops. There are two $d_{x^2-y^2}$ superconducting phases with and without FQ order of O_2^2 . For $J_{22}(\mathbf{0}) = -10t$ and $V_{3z^2-r^2} = 10t$ [Fig. 7(e)], the FQ order is suppressed and $d_{3z^2-r^2}$ superconductivity takes place for $H_{20} > 0$. However the $d_{3z^2-r^2}$ superconductivity is also suppressed by $H_{20} > 0$ and the region of this superconductivity is narrow. Figure 7(f) shows a phase diagram for $J_{22}(\mathbf{0}) = -10t$ with $V_{x^2-y^2} = V_{3z^2-r^2} = 10t$. In the FQ ordered phase of O_2^2 , the system is orthorhombic and the $d_{x^2-y^2}$ and $d_{3z^2-r^2}$ superconductivities can mix. Then, by combining these pairing states, a $d + d$ superconducting phase extends in a wide region.

Finally, we discuss the effects of the uniaxial stress on the coexisting phases of superconductivity with AFQ order. Figure 8(a) is a phase diagram for $J_{20}(\mathbf{Q}) = -10t$ and $V_{x^2-y^2} = 10t$. For $H_{20} < 0$, the AFQ order of O_2^0 is suppressed and T_{SC} increases. However, a negative H_{20} also suppresses the $d_{x^2-y^2}$ superconductivity and T_{SC} does not become high. For $J_{20}(\mathbf{Q}) = -10t$ and $V_{3z^2-r^2} = 10t$ [Fig. 8(b)], for $H_{20} < 0$, the AFQ order of O_2^0 is suppressed and the $d_{3z^2-r^2}$ superconductivity is enhanced. For $J_{20}(\mathbf{Q}) = -10t$ with $V_{x^2-y^2} = V_{3z^2-r^2} = 10t$ [Fig. 8(c)], almost the whole superconducting region is the $d_{3z^2-r^2}$ phase since it is stable for $H_{20} < 0$, where the AFQ order of O_2^0 becomes unstable. For a large H_{20} the $d_{x^2-y^2}$ superconducting phase appears since this superconductivity is cooperative with a positive $O_2^0(\mathbf{0})$.

Figure 8(d) is a phase diagram for $J_{22}(\mathbf{Q}) = -10t$ and $V_{x^2-y^2} = 10t$. For $H_{20} > 0$, the AFQ order of O_2^2 is suppressed and the $d_{x^2-y^2}$ superconductivity develops. For $J_{22}(\mathbf{Q}) = -10t$ and $V_{3z^2-r^2} = 10t$ [Fig. 8(e)], the AFQ order is suppressed and $d_{3z^2-r^2}$ superconductivity takes place for $H_{20} > 0$. However, the $d_{3z^2-r^2}$ superconductivity is also suppressed by $H_{20} > 0$ and T_{SC} remains low. Then, for $J_{22}(\mathbf{Q}) = -10t$ with $V_{x^2-y^2} = V_{3z^2-r^2} = 10t$ [Fig. 8(f)], we obtain the same phase diagram as in Fig. 8(d) within numerical errors.

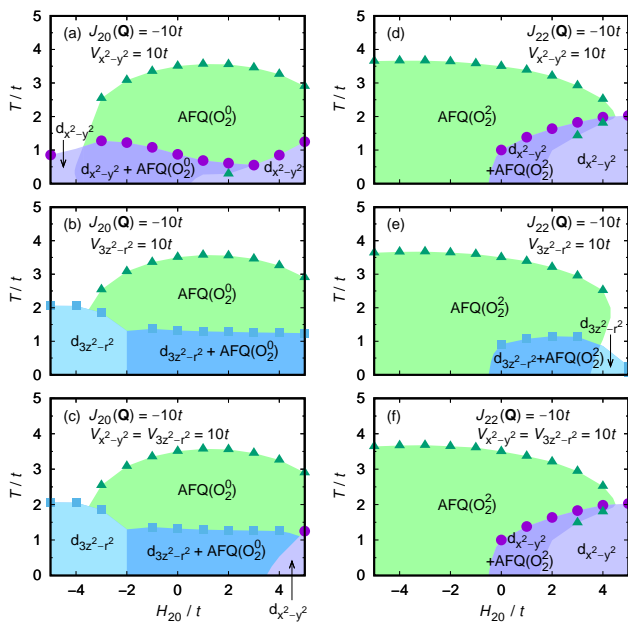


FIG. 8. Phase diagrams of superconductivity coexisting with AFQ order in the H_{20} - T plane: with $J_{20}(\mathbf{Q}) = -10t$ (a) for $V_{x^2-y^2} = 10t$, (b) for $V_{3z^2-r^2} = 10t$, and (c) for $V_{x^2-y^2} = V_{3z^2-r^2} = 10t$; with $J_{22}(\mathbf{Q}) = -10t$ (d) for $V_{x^2-y^2} = 10t$, (e) for $V_{3z^2-r^2} = 10t$, and (f) for $V_{x^2-y^2} = V_{3z^2-r^2} = 10t$.

V. SUMMARY

We have investigated the coexisting phases of the d -wave superconductivity and quadrupole order in a model for the Γ_3 system.

In the d -wave superconducting states, the cubic sym-

metry is broken by the anisotropic pairing and FQ moment of O_2^0 becomes finite except for the $d + id$ superconducting state. Thus, superconductivity can occur cooperatively with the FQ order of O_2^0 . Indeed, the $d_{x^2-y^2}$ superconductivity is enhanced with the help of the FQ order in the present model. It is in sharp contrast to ordinary cases, where superconductivity is suppressed when another order develops. This case may correspond to the superconductivity in $\text{PrTi}_2\text{Al}_{20}$ ^{15,18,20,27-31}.

The other types of quadrupole order are unfavorable for superconductivity. Thus, superconductivity emerges by suppressing the quadrupole order by reducing the quadrupole interaction or by applying uniaxial stress. We could not find a simultaneous transition of superconductivity and AFQ order without fine tuning of parameters. Thus, we need further studies to explain such a transition observed in $\text{PrRh}_2\text{Zn}_{20}$ ³².

The $d + id$ superconductivity does not accompany a quadrupole moment since the cubic symmetry is retained. By lowering symmetry with a uniaxial stress, either of the $d_{x^2-y^2}$ and $d_{3z^2-r^2}$ superconducting transition temperatures rises and at a lower temperature, second superconducting transition breaking time reversal symmetry occurs. Also for the other superconducting states, the superconducting transition temperature and superconducting symmetry can be changed by uniaxial stress.

In any case, the effects of the hydrostatic and uniaxial pressure will be interesting and useful to investigate superconductivity in the Γ_3 systems. Theoretically, a microscopic description of the coexisting states without introducing phenomenological quadrupole interactions is also desirable. It is an important future problem.

¹ W. E. Pickett, Electronic structure of the high-temperature oxide superconductors, *Rev. Mod. Phys.* **61**, 433 (1989).
² E. Dagotto, Correlated electrons in high-temperature superconductors, *Rev. Mod. Phys.* **66**, 763 (1994).
³ K. Ishida, Y. Nakai, and H. Hosono, To What Extent Iron-Pnictide New Superconductors Have Been Clarified: A Progress Report, *J. Phys. Soc. Jpn.* **78**, 062001 (2009).
⁴ G. R. Stewart, Superconductivity in iron compounds, *Rev. Mod. Phys.* **83**, 1589 (2011).
⁵ Y. Ōnuki, R. Settai, K. Sugiyama, T. Takeuchi, T. C. Kobayashi, Y. Haga, and E. Yamamoto, Recent Advances in the Magnetism and Superconductivity of Heavy Fermion Systems, *J. Phys. Soc. Jpn.* **73**, 769 (2004).
⁶ H. von Löhneysen, A. Rosch, M. Vojta, and P. Wölfle, Fermi-liquid instabilities at magnetic quantum phase transitions, *Rev. Mod. Phys.* **79**, 1015 (2007).
⁷ M. Sigrist and K. Ueda, Phenomenological theory of unconventional superconductivity, *Rev. Mod. Phys.* **63**, 239 (1991).
⁸ M. R. Norman, The Challenge of Unconventional Superconductivity, *Science* **332**, 196 (2011).

⁹ T. Takimoto, T. Hotta, T. Maehira, and K. Ueda, Spin-fluctuation-induced superconductivity controlled by orbital fluctuation, *J. Phys.: Condens. Matter* **14**, L369 (2002).
¹⁰ T. Takimoto, T. Hotta, and K. Ueda, Superconductivity in the orbital degenerate model for heavy fermion systems, *J. Phys.: Condens. Matter* **15**, S2087 (2003).
¹¹ K. Kubo and T. Hotta, Orbital-Controlled Superconductivity in f -Electron Systems, *J. Phys. Soc. Jpn.* **75**, 083702 (2006).
¹² K. Kubo and T. Hotta, Superconductivity in f -electron systems controlled by crystalline electric fields, *J. Magn. Magn. Mater.* **310**, 572 (2007).
¹³ H. Kontani and S. Onari, Orbital-Fluctuation-Mediated Superconductivity in Iron Pnictides: Analysis of the Five-Orbital Hubbard-Holstein Model, *Phys. Rev. Lett.* **104**, 157001 (2010).
¹⁴ Y. Yanagi, Y. Yamakawa, and Y. Ono, Two types of s -wave pairing due to magnetic and orbital fluctuations in the two-dimensional 16-band d - p model for iron-based superconductors, *Phys. Rev. B* **81**, 054518 (2010).
¹⁵ M. Koseki, Y. Nakanishi, K. Deto, G. Koseki, R. Kashi-

- wazaki, F. Shichinomiya, M. Nakamura, M. Yoshizawa, A. Sakai, and S. Nakatsuji, Ultrasonic Investigation on a Cage Structure Compound $\text{PrTi}_2\text{Al}_{20}$, *J. Phys. Soc. Jpn.* **80**, SA049 (2011).
- ¹⁶ T. Onimaru, K. T. Matsumoto, Y. F. Inoue, K. Umeo, T. Sakakibara, Y. Karaki, M. Kubota, and T. Takabatake, Antiferroquadrupolar Ordering in a Pr-Based Superconductor $\text{PrIr}_2\text{Zn}_{20}$, *Phys. Rev. Lett.* **106**, 177001 (2011).
- ¹⁷ M. Matsushita, J. Sakaguchi, Y. Taga, M. Ohya, S. Yoshiuchi, H. Ota, Y. Hirose, K. Enoki, F. Honda, K. Sugiyama, M. Hagiwara, K. Kindo, T. Tanaka, Y. Kubo, T. Takeuchi, R. Settai, and Y. Ōnuki, Fermi Surface Property and Characteristic Crystalline Electric Field Effect in $\text{PrIr}_2\text{Zn}_{20}$, *J. Phys. Soc. Jpn.* **80**, 074605 (2011).
- ¹⁸ A. Sakai and S. Nakatsuji, Kondo Effects and Multipolar Order in the Cubic $\text{PrTr}_2\text{Al}_{20}$ ($\text{Tr} = \text{Ti}, \text{V}$), *J. Phys. Soc. Jpn.* **80**, 063701 (2011).
- ¹⁹ I. Ishii, H. Muneshige, Y. Suetomi, T. K. Fujita, T. Onimaru, K. T. Matsumoto, T. Takabatake, K. Araki, M. Akatsu, Y. Nemoto, T. Goto, and T. Suzuki, Antiferro-Quadrupolar Ordering at the Lowest Temperature and Anisotropic Magnetic Field–Temperature Phase Diagram in the Cage Compound $\text{PrIr}_2\text{Zn}_{20}$, *J. Phys. Soc. Jpn.* **80**, 093601 (2011).
- ²⁰ T. J. Sato, S. Ibuka, Y. Nambu, T. Yamazaki, T. Hong, A. Sakai, and S. Nakatsuji, Ferroquadrupolar ordering in $\text{PrTi}_2\text{Al}_{20}$, *Phys. Rev. B* **86**, 184419 (2012).
- ²¹ I. Ishii, H. Muneshige, S. Kamikawa, T. K. Fujita, T. Onimaru, N. Nagasawa, T. Takabatake, T. Suzuki, G. Ano, M. Akatsu, Y. Nemoto, and T. Goto, Antiferroquadrupolar ordering and magnetic-field-induced phase transition in the cage compound $\text{PrRh}_2\text{Zn}_{20}$, *Phys. Rev. B* **87**, 205106 (2013).
- ²² K. Iwasa, H. Kobayashi, T. Onimaru, K. T. Matsumoto, N. Nagasawa, T. Takabatake, S. Ohira-Kawamura, T. Kikuchi, Y. Inamura, and K. Nakajima, Well-Defined Crystal Field Splitting Schemes and Non-Kramers Doublet Ground States of f Electrons in $\text{PrT}_2\text{Zn}_{20}$ ($\text{T} = \text{Ir}, \text{Rh}$, and Ru), *J. Phys. Soc. Jpn.* **82**, 043707 (2013).
- ²³ S. Hamamoto, S. Fujioka, Y. Kanai, K. Yamagami, Y. Nakatani, K. Nakagawa, H. Fujiwara, T. Kiss, A. Higashiya, A. Yamasaki, T. Kadono, S. Imada, A. Tanaka, K. Tamasaku, M. Yabashi, T. Ishikawa, K. T. Matsumoto, T. Onimaru, T. Takabatake, and A. Sekiyama, Linear Dichroism in Angle-Resolved Core-Level Photoemission Spectra Reflecting $4f$ Ground-State Symmetry of Strongly Correlated Cubic Pr Compounds, *J. Phys. Soc. Jpn.* **86**, 123703 (2017).
- ²⁴ T. Onimaru, K. T. Matsumoto, Y. F. Inoue, K. Umeo, Y. Saiga, Y. Matsushita, R. Tamura, K. Nishimoto, I. Ishii, T. Suzuki, and T. Takabatake, Superconductivity and Structural Phase Transitions in Caged Compounds $\text{RT}_2\text{Zn}_{20}$ ($\text{R} = \text{La}, \text{Pr}$, $\text{T} = \text{Ru}, \text{Ir}$), *J. Phys. Soc. Jpn.* **79**, 033704 (2010).
- ²⁵ K. Iwasa, K. T. Matsumoto, T. Onimaru, T. Takabatake, J.-M. Mignot, and A. Gukasov, Evidence for antiferromagnetic-type ordering of f -electron multipoles in $\text{PrIr}_2\text{Zn}_{20}$, *Phys. Rev. B* **95**, 155106 (2017).
- ²⁶ M. Tsujimoto, Y. Matsumoto, T. Tomita, A. Sakai, and S. Nakatsuji, Heavy-Fermion Superconductivity in the Quadrupole Ordered State of $\text{PrV}_2\text{Al}_{20}$, *Phys. Rev. Lett.* **113**, 267001 (2014).
- ²⁷ T. U. Ito, W. Higemoto, K. Ninomiya, H. Luetkens, C. Baines, A. Sakai, and S. Nakatsuji, μSR Evidence of Nonmagnetic Order and ^{141}Pr Hyperfine-Enhanced Nuclear Magnetism in the Cubic Γ_3 Ground Doublet System $\text{PrTi}_2\text{Al}_{20}$, *J. Phys. Soc. Jpn.* **80**, 113703 (2011).
- ²⁸ A. Sakai, K. Kuga, and S. Nakatsuji, Superconductivity in the Ferroquadrupolar State in the Quadrupolar Kondo Lattice $\text{PrTi}_2\text{Al}_{20}$, *J. Phys. Soc. Jpn.* **81**, 083702 (2012).
- ²⁹ K. Matsubayashi, T. Tanaka, A. Sakai, S. Nakatsuji, Y. Kubo, and Y. Uwatoko, Pressure-Induced Heavy Fermion Superconductivity in the Nonmagnetic Quadrupolar System $\text{PrTi}_2\text{Al}_{20}$, *Phys. Rev. Lett.* **109**, 187004 (2012).
- ³⁰ K. Matsubayashi, T. Tanaka, J. Suzuki, A. Sakai, S. Nakatsuji, K. Kitagawa, Y. Kubo, and Y. Uwatoko, Heavy Fermion Superconductivity under Pressure in the Quadrupole System $\text{PrTi}_2\text{Al}_{20}$, *JPS Conf. Proc.* **3**, 011077 (2014).
- ³¹ T. Taniguchi, M. Yoshida, H. Takeda, M. Takigawa, M. Tsujimoto, A. Sakai, Y. Matsumoto, and S. Nakatsuji, NMR Observation of Ferro-Quadrupole Order in $\text{PrTi}_2\text{Al}_{20}$, *J. Phys. Soc. Jpn.* **85**, 113703 (2016).
- ³² T. Onimaru, N. Nagasawa, K. T. Matsumoto, K. Wakiya, K. Umeo, S. Kittaka, T. Sakakibara, Y. Matsushita, and T. Takabatake, Simultaneous superconducting and antiferroquadrupolar transitions in $\text{PrRh}_2\text{Zn}_{20}$, *Phys. Rev. B* **86**, 184426 (2012).
- ³³ K. Kubo and T. Hotta, Influence of lattice structure on multipole interactions in Γ_3 non-Kramers doublet systems, *Phys. Rev. B* **95**, 054425 (2017).
- ³⁴ K. Kubo and T. Hotta, Multipole interactions of Γ_3 non-Kramers doublet systems on cubic lattices, *J. Phys.: Conf. Ser.* **969**, 012096 (2018).
- ³⁵ K. Kubo, Anisotropic Superconductivity Emerging from the Orbital Degrees of Freedom in a Γ_3 Non-Kramers Doublet System, *J. Phys. Soc. Jpn.* **87**, 073701 (2018).
- ³⁶ K. Kubo, Superconductivity in a multiorbital model for the Γ_3 crystalline electric field state, *AIP Adv.* **8**, 101313 (2018).
- ³⁷ K. Kubo, Pairing symmetry in a two-orbital Hubbard model on a square lattice, *Phys. Rev. B* **75**, 224509 (2007).
- ³⁸ L. Fu, Odd-parity topological superconductor with nematic order: Application to $\text{Cu}_x\text{Bi}_2\text{Se}_3$, *Phys. Rev. B* **90**, 100509(R) (2014).
- ³⁹ K. Matano, M. Kriener, K. Segawa, Y. Ando, and G.-q. Zheng, Spin-rotation symmetry breaking in the superconducting state of $\text{Cu}_x\text{Bi}_2\text{Se}_3$, *Nat. Phys.* **12**, 852 (2016).
- ⁴⁰ Y. Pan, A. M. Nikitin, G. K. Araizi, Y. K. Huang, Y. Matsushita, T. Naka, and A. de Visser, Rotational symmetry breaking in the topological superconductor $\text{Sr}_x\text{Bi}_2\text{Se}_3$ probed by upper-critical field experiments, *Sci. Rep.* **6**, 28632 (2016).
- ⁴¹ S. Yonezawa, K. Tajiri, S. Nakata, Y. Nagai, Z. Wang, K. Segawa, Y. Ando, and Y. Maeno, Thermodynamic evidence for nematic superconductivity in $\text{Cu}_x\text{Bi}_2\text{Se}_3$, *Nat. Phys.* **13**, 123 (2017).
- ⁴² T. Asaba, B. J. Lawson, C. Tinsman, L. Chen, P. Corbae, G. Li, Y. Qiu, Y. S. Hor, L. Fu, and L. Li, Rotational Symmetry Breaking in a Trigonal Superconductor Nb-doped Bi_2Se_3 , *Phys. Rev. X* **7**, 011009 (2017).
- ⁴³ K. Yano, T. Sakakibara, T. Tayama, M. Yokoyama, H. Amitsuka, Y. Homma, P. Miranović, M. Ichioka, Y. Tsutsumi, and K. Machida, Field-Angle-Dependent Specific Heat Measurements and Gap Determination of a Heavy Fermion Superconductor URu_2Si_2 , *Phys. Rev. Lett.* **100**, 017004 (2008).

- ⁴⁴ Y. Kasahara, T. Iwasawa, H. Shishido, T. Shibauchi, K. Behnia, Y. Haga, T. D. Matsuda, Y. Onuki, M. Sigrist, and Y. Matsuda, Exotic Superconducting Properties in the Electron-Hole-Compensated Heavy-Fermion “Semimetal” URu₂Si₂, *Phys. Rev. Lett.* **99**, 116402 (2007).
- ⁴⁵ S. Kittaka, Y. Shimizu, T. Sakakibara, Y. Haga, E. Yamamoto, Y. Ōnuki, Y. Tsutsumi, T. Nomoto, H. Ikeda, and K. Machida, Evidence for Chiral d-Wave Superconductivity in URu₂Si₂ from the Field-Angle Variation of Its Specific Heat, *J. Phys. Soc. Jpn.* **85**, 033704 (2016).
- ⁴⁶ R. Nandkishore, L. S. Levitov, and A. V. Chubukov, Chiral superconductivity from repulsive interactions in doped graphene, *Nat. Phys.* **8**, 158 (2012).
- ⁴⁷ M. L. Kiesel, C. Platt, W. Hanke, D. A. Abanin, and R. Thomale, Competing many-body instabilities and unconventional superconductivity in graphene, *Phys. Rev. B* **86**, 020507(R) (2012).
- ⁴⁸ A. M. Black-Schaffer and C. Honerkamp, Chiral d-wave superconductivity in doped graphene, *J. Phys.: Condens. Matter* **26**, 423201 (2014).
- ⁴⁹ J. Goryo, M. H. Fischer, and M. Sigrist, Possible pairing symmetries in SrPtAs with a local lack of inversion center, *Phys. Rev. B* **86**, 100507(R) (2012).
- ⁵⁰ C. W. Hicks, D. O. Brodsky, E. A. Yelland, A. S. Gibbs, J. A. N. Bruin, M. E. Barber, S. D. Edkins, K. Nishimura, S. Yonezawa, Y. Maeno, and A. P. Mackenzie, Strong Increase of T_c of Sr₂RuO₄ Under Both Tensile and Compressive Strain, *Science* **344**, 283 (2014).
- ⁵¹ A. Steppke, L. Zhao, M. E. Barber, T. Scaffidi, F. Jerzembeck, H. Rosner, A. S. Gibbs, Y. Maeno, S. H. Simon, A. P. Mackenzie, and C. W. Hicks, Strong peak in T_c of Sr₂RuO₄ under uniaxial pressure, *Science* **355**, eaaf9398 (2017).
- ⁵² K. Kubo and T. Hotta, Analysis of f - p model for octupole ordering in NpO₂, *Phys. Rev. B* **72**, 132411 (2005).
- ⁵³ T. Hotta and K. Ueda, Construction of a microscopic model for f -electron systems on the basis of a j - j coupling scheme, *Phys. Rev. B* **67**, 104518 (2003).
- ⁵⁴ K. Kubo and T. Hotta, Multipole ordering in f -electron systems on the basis of a j - j coupling scheme, *Phys. Rev. B* **72**, 144401 (2005).
- ⁵⁵ K. Hattori and H. Tsunetsugu, Antiferro Quadrupole Orders in Non-Kramers Doublet Systems, *J. Phys. Soc. Jpn.* **83**, 034709 (2014).
- ⁵⁶ S. Lee, S. Trebst, Y. B. Kim, and A. Paramakanti, Landau theory of multipolar orders in Pr(Y)₂X₂₀ Kondo materials ($Y = \text{Ti, V, Rh, Ir}$; $X = \text{Al, Zn}$), *Phys. Rev. B* **98**, 134447 (2018).
- ⁵⁷ O. Sakai, R. Shiina, and H. Shiba, Invariant Form of Multipolar Interactions and Relation between Antiferro-Quadrupolar Order and Field-Induced Magnetic Moments, *J. Phys. Soc. Jpn.* **72**, 1534 (2003).